



Selective Hydrogenolysis of Biodiesel Waste Bioglycerol Over Titanium Phosphate (TiP) Catalysts: The Effect of Pt & WO₃ Loadings

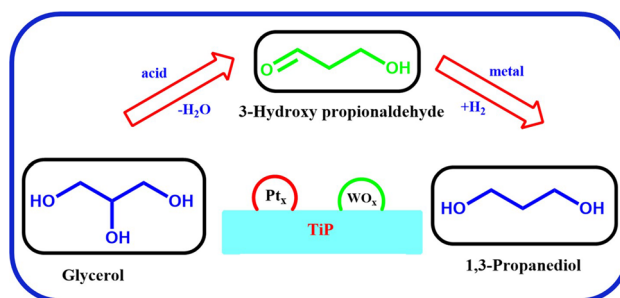
Bhanuchander Ponnala¹ · Putrakumar Balla¹ · S. K. Hussain¹ · Srinivasa Rao Ginjupalli² · Kumaraswamy Koppadi¹ · Nagaraju Nekkala¹ · Vijayanand Perupogu¹ · Ulla Lassi³ · Prem Kumar Seelam³

Received: 14 February 2022 / Accepted: 14 August 2022 / Published online: 7 September 2022
© The Author(s) 2022

Abstract

Glycerol is an important by-product (biowaste) from biodiesel production. Transformation of glycerol into value-added compounds is critical in improving the overall efficiency of the biodiesel production. In this work, a sustainable and cleaner production of 1,3-propanediol (1,3-PDO) by vapor phase hydrogenolysis of glycerol was performed over titanium phosphate (TiP) supported catalysts by varying the Pt and WO₃ loadings (5–20 wt.%). The WO₃ promoted Pt modified TiP catalysts were prepared by a simple wet impregnation method and characterized by various analytical techniques in determining the key properties. Furthermore, the catalyst activity and stability were studied under different reaction conditions. The synergistic effects of Pt and WO₃ loadings on the final performance of the catalyst has been significant in improving the hydrogen transfer rate. Both Pt and WO₃ promotional effects is envisaged the enhanced catalytic properties in conjunction with TiP support acidity. WO₃ incorporation increased Brønsted acidity and formed strong interactions with Pt over TiP support. Both Lewis and Brønsted acid sites presented but BAS played a key role in enhancing the 1,3-PDO selectivity in a bifunctional dehydration-hydrogenation reaction mechanism of glycerol. The effect of reaction temperature, contact times and the weight hour space velocity were evaluated. Overall, under optimized reaction conditions, 2 wt.% Pt-10 wt.% WO₃/TiP catalyst displayed superior activity with a maximum glycerol conversion of ~85% and ~51% of 1,3-PDO selectivity achieved at time on stream of 4 h.

Graphical Abstract



Keywords Glycerol · 1,3-propanediol · Platinum · WO₃ · Titanium phosphates

Statement of Novelty

The novelty and scientific significance of the work is to introduce and to study the promotional effects of Pt and WO₃ over titanium phosphate-based catalysts and which is quite new in this area. Both Pt and tungsten had significant role in gaining the highest selectivity and activity in glycerol

✉ Putrakumar Balla
bputrakumar@yahoo.com

✉ Prem Kumar Seelam
prem.seelam@oulu.fi

Extended author information available on the last page of the article

conversion to 1,3-PDO. Especially, WO_3 avoid the side reactions and improve the selective formation of 1,3-PDO and also reduce the carbon formation.

Introduction

The depletion of conventional energy reserves and growing environmental problems made pursuing sustainable energy production as key solution. Apparently, alternative bio-based fuels and chemicals are emerging as the long-term solution [1]. Glycerol is a simple chemical intermediate from biomass conversion and a trihydroxy molecule with over 2000 known applications in various industries and a potential by-product from the biodiesel production. Globally, biodiesel is a promising alternative to the fossil-based fuel and also one of the future sustainable fuels and typically produced by transesterification of vegetable oils with methanol under basic conditions [2–5]. With the rapid development of the biodiesel industry, a large amount of crude glycerol is being formed as byproduct, around global production of six million tons by 2025 [6]. There is a challenge in utilizing large amounts of bioglycerol efficiently and thus, has a great impact on the overall economics of the biodiesel production plants. In this context, valorization of glycerol in the production of high value-added polymer precursors, chemicals and fuel additives was found to be an important alternative to improve the overall techno-economic viability. One of the most promising routes of upgrading the glycerol is to produce 1,3-propanediol (1,3-PDO) via catalytic hydrogenolysis [7]. There is a great demand for 1,3-PDO for industrial applications and producing 1,3-PDO environmentally benign methods using renewable feedstocks is crucially important. Generally, 1,3-PDO is a valuable polymer precursor and an intermediate compound with a wide variety of industrial applications such as in coatings, adhesives, composites, carpet and textile manufacturing, cosmetics, and personal and home appliances. It is mostly used as a building block in the synthesis of polytrimethylene terephthalate polymer (PTT).

Generally, glycerol hydrogenolysis to PDOs reaction exhibit three different mechanisms, first being the dehydration-hydrogenation route, second is the dehydrogenation-dehydration-hydrogenation route and the third being the direct glycerol hydrogenolysis pathway as reported in [5, 7–10]. The three mechanisms solely depends on the type of active phase, catalyst composition, reaction conditions and the support acidity. In the first step, the glycerol undergoes dehydration over acid sites of the support. In the next step, hydrogenation occurs over the catalyst's metal sites (active phase) to produce 1,2-propanediol and 1,3-propanediol, respectively. In the direct glycerol hydrogenolysis, the active

H_2 species forms the hydride attack on -OH group and then successive formation of PDOs occur [7–9].

The hydrogenolysis of glycerol has been studied over different heterogeneous supported catalysts such as Ru/TiO₂, Pt/mordenite, Pt-Cu/H-mordenite, Rh-ReO_x/SiO₂, Ir-ReO_x/SiO₂, and Pt/S-MMT catalysts [11–17]. The non-noble metal catalysts such as Cu, Ni and Co-based catalysts are also studied extensively in glycerol hydrogenation to 1,3-PDO. Further, Cu-based catalysts have shown promising results in 1,3-PDO production but exhibit low stability and prone to faster deactivation via Cu agglomeration. Among the noble metals, Pt-based catalysts shown highest activity and thermal stability towards glycerol hydrogenolysis [18]. Moreover, many studies preferred Pt-based catalysts in the selective production of 1,3-PDO than the other transition metal-based catalysts. Glycerol hydrogenolysis involves a complex mechanism and it involves a bifunctional pathway in the formation of 1,3-PDO. As previously studied, 1,2-PDO formation is less complex and relatively easy than 1,3-PDO formation via glycerol hydrogenation. In 1,3-PDO formation, two key catalytic functionalities are required that is balanced support acidity for dehydration (abstraction of -OH group to -H₂O) and the active metal sites for hydrogenation-rearrangement of -OH mechanism. In addition, support acidity type (Lewis-Bronsted), strength, and the amount will have greater influence on the activity. The structure–activity and acidity–activity are key correlations made in glycerol hydrogenolysis. Samudrala et al. 2018, studied C-O hydrogenolysis of glycerol over Pt/S-MMT catalysts by varying the Pt loadings (0.5–3 wt.%) [14]. The sulphuric acid activated and optimal 2 wt.% Pt/S-MMT catalyst exhibited highest activity and selectivity for 1,3-PDO due to the incorporation of Brønsted acidity and well-dispersed Pt nanoparticles. Nevertheless, dispersion and acidity-basicity correlation has been salient features in many catalytic reactions. Over 2 wt.% Pd/Mo-Al catalyst gained over 90% activity with 91% toward total propanol selectivity at 210 °C. The weak to moderate acid sites of the catalyst system influenced the degree of glycerol dehydroxylation to accelerate glycerol dehydration to 1-propanol and 2-propanal [19]. Similarly, the effect of WO_x promoter on the selective formation of 1,3-PDO was studied over Pt-WO_x/Al₂O₃ catalysts. The bifunctionality of Pt and WO_x was delivered different activities, and this solely depends on the WO_x content. An optimal 10 wt.% WO_x promoter exhibited best results in yielding 42% of 1,3-PDO due to the high amount of Brønsted acid sites (BAS), strong electronic interaction between Pt-WO_x and hydrogen spillover [20]. Henceforth, BAS is highly correlated with selective formation of 1,3-PDO, whereas Lewis acid sites predominantly participate in 1,2-PDO formation. Nevertheless, the ratio of BAS to LAS can also be critical factor in obtaining highest activity in selective formation of 1,3-PDO [20]. In Chary et al. [24], studied the selective hydrogenation of glycerol

to 1,3-propanediol over 2 wt.% Pt-10WO₃/SBA-15 catalyst and gained moderately high 1,3-PDO selectivity (~42%). Typically, the selective production of 1,3-PDO from glycerol involves two reaction steps (Scheme 1): first dehydration of glycerol to 3-hydroxypropanal over acidic sites and, next step hydrogenation of 3-hydroxypropanal to 1,3-PDO over metallic sites [25]. Therefore, co-existence of metal sites with optimal total acid sites is key for the selective production of 1,3-PDO. The platinum metal is a promising catalyst for oxidation and hydrogenation reactions. Moreover, Pt is known for being active and selective towards C–O and C–C bond scissions and cleavages (Scheme 1). For example, as reported earlier, Pt is known for the highly active phase in 3-hydroxypropanal hydrogenation [25].

Recently, we found few studies reported on Pt-WO_x based catalysts supported over different support materials. The C–O bond dissociation in C₃ polyols occurs either on primary or secondary carbons depending on the support and active phase. Over Pt-WO₃/Al₂O₃ catalyst, hydrogenolysis rate was higher at secondary carbon than primary [21]. The -OH group at primary carbon influenced by the bond cleavage of C–O at secondary carbon. Thus, the position and structure of the substrate over the catalyst surface must be controlled for selective hydrogenolysis of glycerol.

In Zhu et al., a series of Pt–yLi₂B₄O₇/WO_x/ZrO₂ (y = 0–2 wt.%) catalysts were synthesized by changing the Li₂B₄O₇ content. Overall, the 1 wt.% Li₂B₄O₇ exhibited the highest activity with 91% glycerol conversion and possessed excellent stability than other counter parts. The Li borate improved the activity of Pt-WO_x/ZrO₂ by enhancing the Pt dispersion and by increasing total surface acidity [20]. In another study conducted in a fixed bed reactor at 160 °C over Pt-WO_x/Al₂O₃ catalyst, a 75.2% of glycerol conversion was achieved due to better interactions between Pt & WO_x and improved Pt dispersion in the creation of active sites [22]. As reported in *Da Silva Ruy* et al., review on glycerol hydrogenolysis to 1,3-PDO and focused on Pt and Pt-WO_x based catalytic systems [23]. As the start of art is more focused on Pt, Cu and Ir-based catalysts with promoters and additives in combination with WO_x can greatly influence the selective glycerol hydrogenation. In another study by Zhou et al. investigated WO_x modified Pt-WO_x/ZrO₂ catalysts, and the high WO_x polymerization degree was created by doping optimal Mn content [22]. In addition, the polymerized WO_x domains had strong interactions with Pt and formed strong super Bronsted acid sites *i.e.*, Pt-(WO_x)_n-H through secondary adsorbed surface -OH groups.

However, the reported selectivity and yields in the literature of 1,3-PDO is relatively low due to the formation of by-products in the similar temperature range. Thus, further studies are conducted to modify the Pt-based catalysts through the addition of promoters and secondary metals to improve the selective formation of 1,3-PDO. Thus, in this

work, we modified titanium phosphate support materials with active phases *i.e.*, WO_x and Pt. We varied the Pt and WO_x loadings to determine the optimized active phases in glycerol to 1,3-PDO. Understanding the effect of Pt and WO_x in glycerol conversion was evaluated.

Experimental Section

Materials and Methods

The list of chemical reagents and solvents used in the study are chloroplatinic acid hexahydrate (H₂PtCl₆·6H₂O, Sigma-Aldrich), Ammonium metatungstate hydrate ((NH₄)₆(H₂W₁₂O₄₀)·H₂O) (85%) (Sigma-Aldrich), Titanium n-butoxide (TBT) (98%) (Avra Synthesis Pvt. Ltd), and n-butanol (99.7%) (Sigma-Aldrich), 0.1 M phosphoric acid (86%) (Avra Synthesis Pvt. Ltd), deionized water, all chemical reagents were commercially available in analytical purity and used without further purification.

Preparation of TiP Support

In a modified hydrothermal process, titanium phosphate (Ti₃P₄O₁₆, TiP) was synthesized by using a mixture of n-butanol and titanium n-butoxide (TBT) compounds to which 30 mL of 0.1 M phosphoric acid (H₃PO₄) solution was added drop-wise and kept under stirring for 2 h at room temperature. The resulted mixture was dried and aged for 24 h at 80 °C in a Teflon-lined autoclave reactor. In the next step, the solid precipitated product was filtered and washed several times with deionized water. Finally, the material was dried at 60 °C for 12 h and then calcined at 500 °C for 2 h.

Preparation of Pt-WO₃/TiP Catalysts

The precursors of platinum and tungsten are chloroplatinic acid hexahydrate (H₂PtCl₆·6H₂O) and ammonium metatungstate hydrate ((NH₄)₆(H₂W₁₂O₄₀)H₂O) were used, respectively. The catalysts were prepared by sequential impregnation methods with target loadings. At first, the titanium phosphate (TiP) support was impregnated with ammonium metatungstate hydrate ((NH₄)₆(H₂W₁₂O₄₀)H₂O) precursor solution, and subsequently, the introduction of Pt salt solution was impregnated in the next step. The resulting solids were dried at 110 °C for 24 h and then calcined at 500 °C for 3 h in air after each impregnation step. The nominal loadings of Pt 2 wt.% and WO₃ (5–20 wt.%) were impregnated with TiP support, respectively. A series of catalysts with Pt loadings (0.5–3 wt.%) over 10WO₃/TiP were prepared by wet impregnation method using aqueous chloroplatinic acid hexahydrate solution. The samples were dried at 110 °C in oven for 12 h and finally calcined at 500 °C for 3 h in air.

Table 1 Catalytic properties of Pt-WO₃/TiP catalysts

Catalyst	BET surface area ^a (m ² /g)	Total pore volume ^a (cc/g)	pore diameter ^a (nm)	Total acidity ^b (μmol/g)
Pure TiP	252.0	0.31	8.41	157
10WO ₃ /TiP	204.5	0.27	8.65	175
2Pt-5WO ₃ /TiP	180.5	0.25	9.63	200
2Pt-10WO ₃ /TiP	165.2	0.20	12.08	210
2Pt-15WO ₃ /TiP	152.6	0.18	15.04	195
2Pt-20WO ₃ /TiP	130.7	0.10	17.52	186

^aResults from N₂ sorption isotherms

^bResults from NH₃-TPD

Catalyst Characterization

The phase and structural analysis of synthesized catalysts was characterized by powder X-ray diffraction (XRD) analysis over a Rigaku miniflex X-ray diffractometer using Ni filtered Cu K α radiation ($\lambda=0.15406$ nm). The textural properties such as the Brunauer–Emmet–Teller (BET) surface area, pore volume and average pore diameter of the catalysts were measured by nitrogen adsorption–desorption isotherms (physisorption) at -196 °C using Autosorb 1 (Quanta chrome instruments).

In pyridine adsorbed FTIR analysis, at first, the catalysts were pretreated in N₂ flow at 300 °C for 1 h to remove moisture and followed by adsorption of pyridine (py) at 120 °C until saturation was achieved. The sample was cooled down to room temperature after pyridine adsorption. Each sample was grounded with KBr, and pressed into the sample holder, and mounted in the cavity of the spectrometer. The FTIR spectra were then recorded on GC-FT-IR Nicolet 670 spectrometer in the spectral range of 1400–1800 cm⁻¹ using KBr as a background spectrum.

The NH₃-TPD experiments were performed on a Auto-Chem 2910 instrument (Micromeritics, USA) equipped with a TCD detector and monitored the desorbed ammonia continuously from the sample. Prior to the TPD measurements, a 0.1 g of sample was dried under helium flow around 50 mL min⁻¹ at 200 °C for 1 h, in the next step, the adsorption of ammonia was performed using a mixture of 10 vol.% NH₃/He at 80 °C for 1 h until saturation point reached. In next step, subsequently flushed with inert flow of 50 mL min⁻¹ for 30 min. The TPD analysis was carried out in the range of 100 °C to 800 °C at a heating rate of 10 °C min⁻¹ and the amount of desorbed NH₃ was measured by using GRAMS/32 software.

Transmission electron microscopy (TEM) analysis was done using JEOL 2010 electron microscope instrument operating at 200 kV. First, the catalyst sample in powder form

was ultrasonicated in ethanol and then dispersed on a carbon coated copper grid. The specimen with the sample was introduced into the microscope column, which was then evacuated under 10⁻⁶ Torr. The scanning electron microscopy (SEM) analysis of morphology and structural images were taken on a Philips Fei Quanta 200 F instrument operated at 20 kV. The Carbon-Hydrogen–Nitrogen–Oxygen (CHNO) elemental analysis of the samples was analyzed using a Horiba EMGA 930 instrument using a calibration method and standard compound with a standard deviation $\pm 3\%$.

Catalyst Activity Testing

The vapor phase glycerol hydrogenolysis was performed in a vertical aligned fixed-bed quartz reactor with 40 cm length and 9 mm internal diameter operated at atmospheric pressure. Before the reaction, a 0.5 g of catalyst was activated and reduced under an H₂ flow of 30 mL min⁻¹ at 350 °C for 2 h. The reactor was cool down to 210 °C reaction temperature under hydrogen flow (30 mL min⁻¹) and the light-off tests were also performed. Further, an aqueous solution of 10 wt.% glycerol *i.e.*, glycerol solution flow rate of 1 mL min⁻¹ was introduced into the reactor inlet through an evaporation zone (glycerol vaporized before entering the reactor). After the reaction test, the products were condensed in an ice trap at 0 °C, and the reactor outlet stream was collected for every hour and analyzed by using gas chromatography (GC-2014, Shimadzu) equipped with DB-wax 123–7033 (Agilent) capillary column (0.32 mm i.d. & 30 m long) equipped with a flame ionization detector (FID). The mass and carbon balances was calculated in each experiment and found the error under ± 5 –8% and the overall, experiments presented a 92–95% confidence interval. Considering the factor of carbon deposition during the reaction test, there is a small change in C balance.

The conversion of glycerol (Eq. 1) and selectivity of products (Eq. 2) were calculated according to the following equation:

$$\text{Conversion}(\%) = \frac{C - \text{based moles of introduced substrate} - C - \text{based moles of remained substrate}}{C - \text{based moles of introduced substrate}} \times 100 \quad (1)$$

$$\text{Selectivity (liquid products)}(\%) = \frac{C - \text{based moles of product}}{\sum C - \text{based moles of all products}} \times 100 \quad (2)$$

Results and Discussion

Characterization of Catalyst

X-ray Diffraction (XRD)

The Fig. 1 display the X-ray diffraction patterns of pure titanium phosphate (TiP), 10WO₃/TiP and 2Pt-xWO₃/TiP (x=5–20 wt.%) phases with different WO₃ loadings. The XRD patterns confirmed that the broad peaks in the range of 15–38° are assigned to the amorphous nature of TiP support. The amorphous nature of the titanium phosphate is consistent and similar to the results reported by Bhaumik et al. [26]. In Fig. 1, the 2Pt-xWO₃/TiP catalysts with WO₃ loadings lower than 10 wt.% content don't exhibit any peak indicating the presence of well-dispersed amorphous WO₃ phases and the catalysts above 10 wt.% loadings, presented a sharp crystalline peak of WO₃. Thus, it is evident that at higher loadings above 10 wt.%, highly crystalline phases of WO₃ are formed.

The additional peaks were observed for the catalysts with 15 wt.% WO₃ loadings and above *i.e.*, in the 2θ region of 23.08°, 23.58°, 24.26°, 26.54°, 28.75° and 33.28° are characteristic peaks of monoclinic phases of WO₃ [18]. Moreover, the XRD patterns also showed three sharp diffraction

peaks around 39.7°, 46.3° and 67.7°, which can be assigned to (111) (200) and (220) lattice planes of Pt (Ref. pattern.00-001-1311) [27]. The intensity of these peaks in platinum loaded catalysts decreased with tungsten loadings, thus, it is a clear indication that the bulk WO₃ covered the Pt species at higher WO₃ loadings. Probably at lower WO₃ loadings exhibit stronger and better interactions with Pt over TiP scaffold. Thus, the phase variation is evident with varied WO₃ loadings.

BET Surface Area and Pore Size Distribution

The textural properties such as surface area, total pore volume, pore size distribution and pore diameter were presented in Table 1 and in SI. The surface area and pore volume of pure TiP is 251 m² g⁻¹ and 0.31 cc g⁻¹, respectively. Whereas the metal impregnated TiP samples presented a reduced surface area in the range of 204–130.7 m² g⁻¹ and pore volume in the range of 0.27 to 0.10 cm³ g⁻¹. From the analysis, it is observed that the impregnation of WO₃ and platinum over TiP support decline both the surface area and pore volume compared to the pure TiP support. It is probably the WO₃ & Pt species that block the mesopores of the pure TiP support. However, the pore diameter increases with the active phase loadings over the support. The isotherms of TiP-based catalysts exhibited a mesoporous materials nature with a characteristic of type IV and indicating a moderate pore size around 8–18 nm with narrow pores. For more details of physisorption of N₂ and pore size distribution of single pore diameter reported in supplementary information (SI).

Scanning Electron Microscopy (SEM)

SEM analysis of 2Pt-xWO₃/TiP catalysts with different WO₃ loadings has been carried out to analyze the morphology and surface topology of the catalysts and the results are displayed in Fig. 2. The SEM analysis of 2Pt-xWO₃/TiP materials showed different structural variations and micron-sized uneven-shaped particles were formed. Moreover, the WO₃ at higher loadings and probably the formation of bulk species over TiP support might be possible (this phenomenon is not confirmed from SEM).

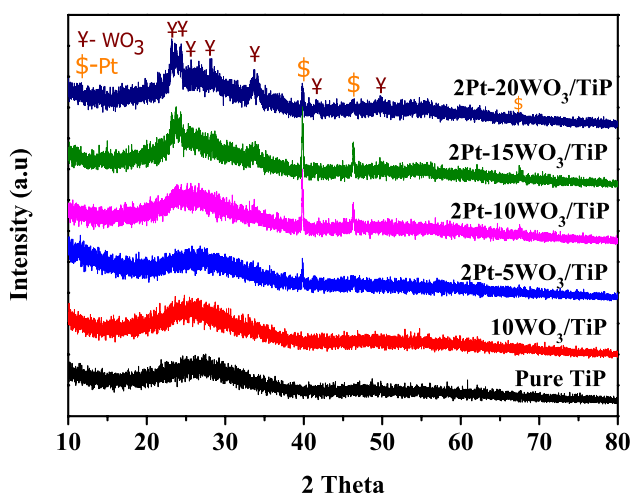


Fig. 1 XRD patterns of pure TiP support, 10WO₃/TiP and 2Pt-xWO₃/TiP catalysts (x=5–20 wt.%)

Table 2 Effect of tungsten loadings on hydrogenolysis of glycerol to 1,3-PDO

Catalyst	X_{Gly}	$S_{1,3\text{-PDO}}$	$S_{1,2\text{-PDO}}$	S_{HA}	S_{Propanol}	S_{Others}
2Pt-5WO ₃ /TiP	63	42	18	15	20	5
2Pt-10WO ₃ /TiP	85	51	14	11	16	6
2Pt-15WO ₃ /TiP	81	46	16	9	24	5
2Pt-20WO ₃ /TiP	69	37	19	15	22	7

Reaction conditions: 0.5 g catalyst, 2Pt-xWO₃/TiP catalyst (x = 5 to 20 wt%); Reaction temperature: 210 °C, H₂ flow rate: 30 mL/min, WHSV = 2.37 h⁻¹, 1,3-propanediol (S_{1,3-PDO}), 1,2-propanediol (S_{1,2-PDO}), Hydroxyacetone (S_{HA}), 1-Propanol, 2-Propanol (S_{Propanol})

Transmission Electron Microscopy (TEM)

The TEM images of 10WO₃/TiP and 2Pt-10WO₃/TiP catalysts are presented in Fig. 3. The morphology of platinum and tungsten particles is determined by using TEM analysis. It can be clearly seen that the tungsten species are uniformly distributed over the support structure in both the samples. Moreover, the dark black spots in the TEM image of 2Pt-10WO₃/TiP represent the platinum particles evenly distributed over the 10WO₃/TiP support. The Pt predominantly presented as smaller fine nanoparticles in the vicinity of WO_x species.

Temperature Programmed Desorption of Ammonia (NH₃-TPD)

The NH₃-TPD method is a useful tool and provides information on the total acidity and strength of the acid sites of the solid materials. The total acidity of the catalysts increased

Fig. 2 SEM images of **a** pure TiP support, **b** 10WO₃/TiP, **c** 2Pt-5WO₃/TiP, **d** 2Pt-10WO₃/TiP, **e** 2Pt-15WO₃/TiP and **f** 2Pt-20WO₃/TiP catalysts

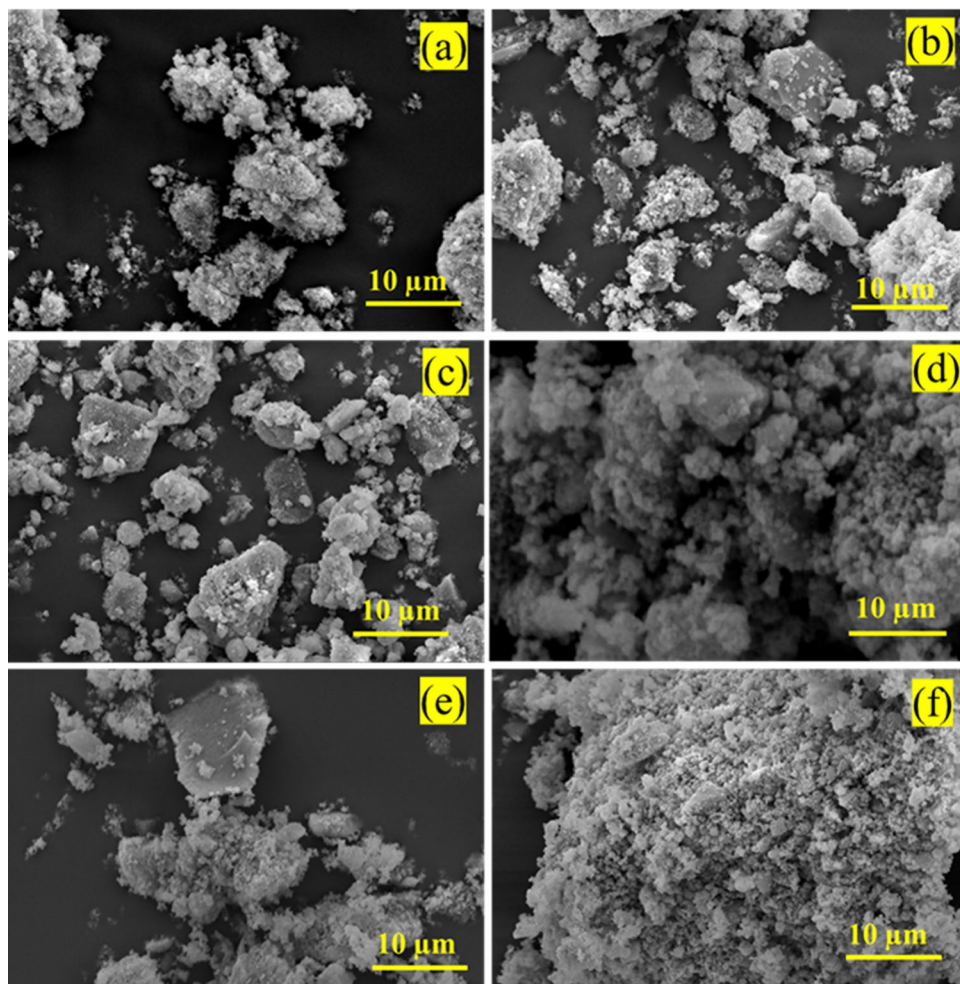
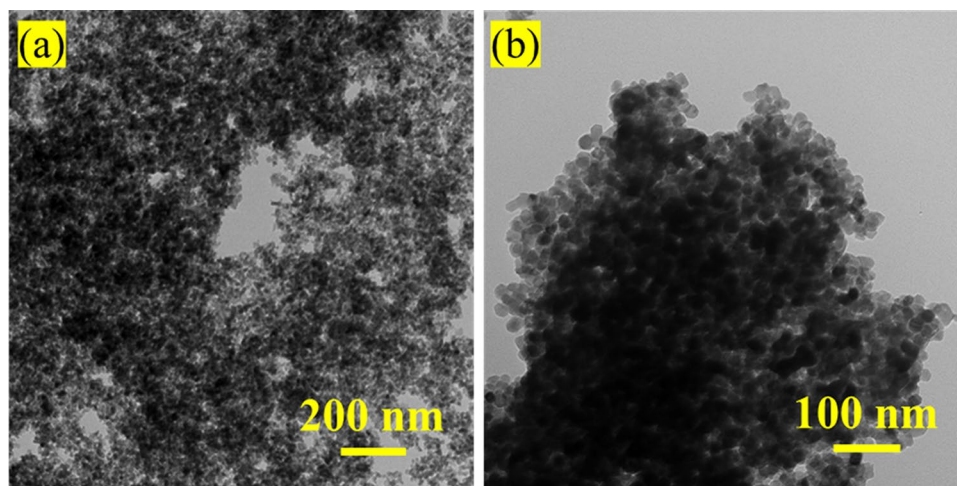


Fig. 3 TEM images of **a** 10WO₃/TiP and **b** 2Pt-10WO₃/TiP catalysts



with the incorporation of WO₃ into TiP support at lower loadings *i.e.*, 5 and 10 wt%. Whereas the surface acidity decreased at higher loadings *i.e.*, 15 and 20 wt%, this might be due to the condensation of W-OH groups and the formation of 3-D WO_x clusters, which finally reduce the total acidity at higher loadings [26]. Typically, TiP possesses acidity generated from protonated tetrahedral units of TiO₄ and PO₄. The acidity of WO₃/TiP catalysts is created due to the presence of surface P-OH groups and well-dispersed WO₃ particles over the TiP surface, which are responsible for the acid sites (both LAS & BAS). The ammonia TPD analysis suggested that the amount of total acidity & strength of acid sites increased with the addition of WO₃ to the TiP support (Table 1). Thus, it is evident that the influence of WO₃ had a significant role in the strength, type and total amount of acidity.

The NH₃-TPD desorption profiles of all catalysts with varied WO₃ loadings are shown in Fig. 4. Typically, the ammonia TPD peaks are divided into three acid sites strength depending on the desorption temperature. The weaker acid sites are in the region of 150–300 °C, moderate acid sites around 300–450 °C and stronger acid sites above 450 °C, respectively [13]. As can be seen from Fig. 4, NH₃-TPD profiles exhibited only two peaks for all the samples. The TPD profile of pure TiP catalyst showed a weaker acid site peak region at 70–160 °C, whereas Pt & WO₃ doped Pt-xWO₃/TiP catalysts exhibited two peaks *i.e.*, a weak acid site peak at 70–160 °C and a broad peak in strong acid site at 450–550 °C.

Pyridine FTIR

Pyridine FTIR analysis is a useful tool in probing the nature of acidity and quantifying the acid sites. Generally, pyridine FTIR analysis confirms that the IR bands that appeared at 1540–1548 cm⁻¹ are assigned to Brønsted acid sites (BAS) and the bands at 1445–1460 cm⁻¹ are assigned to Lewis acid

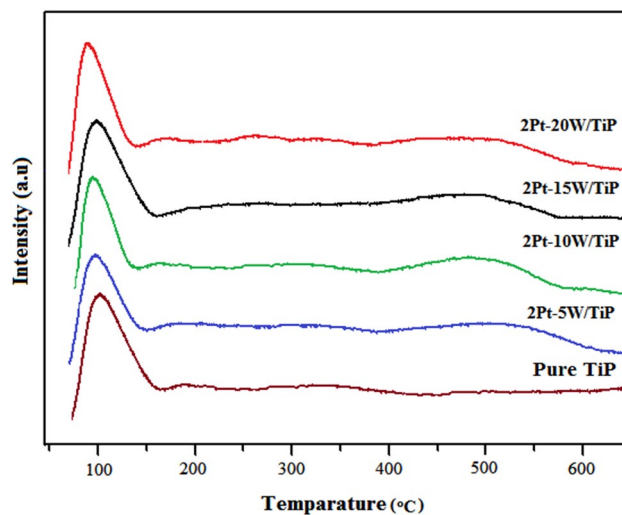


Fig. 4 Results of NH₃-TPD profiles of different WO₃ loaded 2Pt-xWO₃/TiP catalysts

sites (LAS) and the additional IR bands at 1490–1500 cm⁻¹ corresponds to the combination of both Lewis and Brønsted acid sites [28], 26. Generally, pure TiP support exhibits a combination of both LAS & BAS originating from tetrahedral units of TiO₄ and PO₄ framework. Lewis acid sites originated from Ti⁺⁴ species and P-OH (P⁺³OH⁻) units contribute to BAS formation.

Figure 5 represents the pyridine adsorbed FTIR spectra of pure TiP and Pt-xWO₃/TiP (x = 5–20 wt.%) catalysts in the region of 1400–1600 cm⁻¹ bands. All the catalysts possess Brønsted acid sites (BAS), and they appear at 1545 cm⁻¹. Moreover, the combination of both Lewis and Brønsted acid sites (L + B) was observed at 1490 cm⁻¹ and Lewis acid sites (LAS) appeared at 1445 cm⁻¹ band, as shown in Fig. 5. It is evident that with WO₃ loadings from 5 to 20 wt.%, the intensity of IR absorption peak corresponding to the Lewis acidity

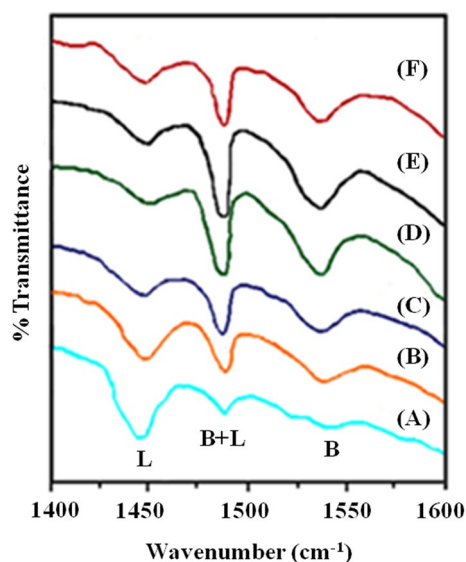


Fig. 5 Pyridine adsorption FTIR profiles of pure TiP and Pt- x WO₃/TiP catalysts. **a** Pure TiP **b** WO₃-TiP **c** Pt-5WO₃/TiP **d** Pt-10WO₃/TiP **e** Pt-15 WO₃/TiP and **f** Pt-20 WO₃/TiP

decreases moderately and the intensity for Brønsted acidity varies. The Lewis acid sites of TiP support tends to decline by incorporating WO_x species. Further, the combination of both Lewis and Brønsted acid sites increased with WO₃ loadings up to 10 wt.% and thereafter, slightly decreased for WO₃ loadings above 10 wt.%. The incorporation of WO_x oxide species forms surface W-OH groups which enhance the BAS. At lower WO₃ loadings *i.e.*, 10 wt.% or below, the Brønsted acidity of WO₃/TiP catalysts increased and after that, declined due to condensation of surface ⁻OH groups. Thus, the WO₃ with 10 wt.% loaded catalyst exhibited the highest amount of total acidity and BAS compared to other catalysts.

Catalytic activity results

Effect of WO₃ and Pt loadings

The effect of WO₃ loadings (5 to 20 wt.%) with 2 wt.% Pt over TiP support in gas phase hydrogenolysis of glycerol was tested and the results are summarized in Table 2. The

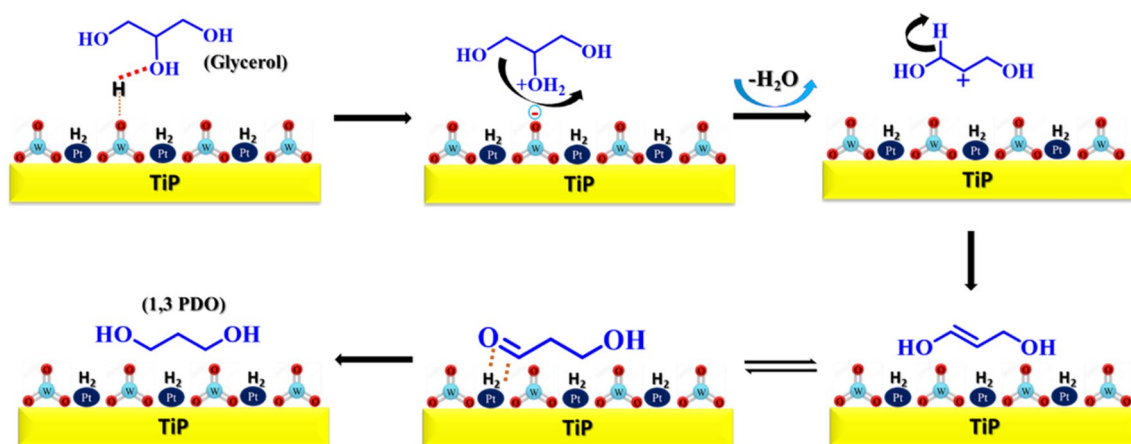
results clearly confirm that the introduction of WO₃ over TiP supported catalysts are more active compared to pure TiP support. Both glycerol conversion and 1,3-PDO selectivity increased from 63 to 85% and 42% to 51%, respectively, with the addition of 5 and 10 wt.% WO₃ loadings. Whereas the activity of the catalysts decreased with WO₃ loadings above 10 wt.% (*i.e.*, 15 and 20 wt.%). The incorporation of WO₃ into TiP support significantly affected the overall catalytic properties and presented a higher selectivity towards 1,3-PDO due to the creation and enhancement of Brønsted acid sites (Scheme 1). The Scheme 1 illustrates the direct glycerol hydrogenolysis via hydride attack which is confirms from the products formation. The surface acidity declined with the bulk formation of WO_x species at higher loadings and condensation of surface-OH groups disappeared due to bulk WO_x. The WO_x undergoes a series of reduction during the hydrogenation mechanism to form more active W-OH centers. Both Bronsted (BAS) and Lewis acidity (LAS) play an important role; however, BAS is more favorable for selective formation of 1,3-PDO [23]. A similar phenomenon was observed to optimise the WO₃ loading by Jarauta-Córdoba et al., 2021 [29]. The structure-acidity correlation was determined and both LAS and BAS are relevant in the selective production of 1,3-PDO. Moreover, the BAS enhanced with WO₃ loadings and influenced the acidity towards secondary C–O bond dissociation and hydrogenation but optimization of WO₃ is vital in obtaining favorable acid sites [29]. Overall, the 10 wt.% WO₃ doped catalyst displayed the highest activity in terms of glycerol conversion and selectivity toward the 1,3-PDO compared to all other tested catalysts (Table 3). We also tested the bare support without Pt *i.e.*, 10 wt.% WO₃-TiP support. Relatively low conversion of 41% with 14% 1,3-PDO selectivity was achieved, which clearly indicates without Pt active phase an H₂ spill-over WO₃ is inefficient and leads to undesirable other hydrogenated by-products (Table 3).

The influence of Pt loadings over hydrogenolysis of glycerol and the final catalytic properties were determined with the series of x Pt-10WO₃/TiP catalysts with different platinum loadings ($x=0.5$ to 3 wt.%). From Table 3, the effect of Pt is also significant in terms of activity and selectivity was displayed. Over the bare support (10WO₃/TiP) shown the

Table 3 Effect of platinum loadings over glycerol hydrogenolysis to propanediols and other byproducts

Catalyst	X _{Gly}	S _{1,3-PDO}	S _{1,2-PDO}	S _{HA}	S _{Propanol}	S _{Others}
10WO ₃ -TiP	41	14	7	39	19	21
0.5Pt-10WO ₃ /TiP	60	35	13	18	26	8
1Pt-10WO ₃ /TiP	72	46	15	13	21	5
2Pt-10WO ₃ /TiP	85	51	14	11	16	6
3Pt-10WO ₃ /TiP	79	48	11	13	19	9

Reaction conditions: 0.5 g catalyst, x Pt-10WO₃/TiP catalyst ($x=0.5$ to 3.0 wt%), Reaction temperature: 210 °C, H₂ flow rate: 30 mL/min, 1,3-propanediol (S_{1,3-PDO}), 1,2-propanediol (S_{1,2-PDO}), Hydroxyacetone (S_{HA}), 1-Propanol, 2-Propanol (S_{Propanol})



Scheme 1 The possible direct glycerol hydrogenolysis reaction mechanism over Pt-WO₃/TiP based catalysts and the role of Pt and WO₃ in creation of hydrogenation sites provided by Pt and Brønsted acid sites (BAS) by WO₃ in conjunction with TiP support

41% conversion of glycerol and 14% selectivity to 1,3PDO was observed. After the addition of Pt, the conversion and selectivity to 1,3 PDO is increased. The effect of Pt is significant in terms of activity and selectivity. The conversion of glycerol from 60 to 85% and selectivity of 1,3-PDO from 35 to 51%, were enhanced with Pt loading and overall, it was found that the most optimal loading is 2 wt. % Pt.

However, both glycerol conversion and 1,3-PDO selectivity decreased slightly over 3 wt.% Pt-10WO₃/TiP catalyst, which might be that the Pt particles block the acid sites, and this was clearly noticed from the XRD results. The other hydrogenated reaction by-products are 1-propanol and 2-propanol are formed in higher amounts and 1,2-PDO was formed in a lower amount. Therefore, among the series of tested catalysts (0.5 to 3 wt% Pt-10WO₃/TiP), the catalyst with 2 wt.% platinum loading (2Pt-10WO₃/TiP) was found to be the best and optimal in exhibiting the highest conversion and selectivity to 1,3-PDO.

Effect of reaction temperature

To study the influence of reaction temperature on the glycerol conversion and products selectivity, the reaction was carried out in a temperature range of 170–250 °C under atmospheric pressure over most optimized 2Pt-10WO₃/TiP catalyst, and the results are illustrated in Fig. 6. As the temperature increases from 170 °C to 250 °C, the glycerol conversion increases monotonically from 69 to 90%. As predicted, conversion typically increases with reaction temperature due to C–O bond dissociation in glycerol molecules. However, the highest 1,3-PDO selectivity of 51% was achieved at 210 °C reaction temperature. Moreover, the selectivity of 1,3-PDO decreased with a further increase in temperature. A similar trend was observed in the 1,2-PDO selectivity whereas a gradual decrease in the selectivity

of Hydroxyacetone (HA) and propanols was observed. At higher temperatures (*i.e.*, > 210 °C), the formation of the by-product such as ethanol, methanol, ethylene glycol and acetone are relatively higher due to subsequent faster C–C cleavage reactions occurring at higher temperatures [30–32]. Most of the reported studies in literature on glycerol hydrogenolysis was performed in a similar temperature range (180–250 °C) but at an elevated H₂ partial pressure over 0.1 MPa.

Effect of contact time

The effect of contact times on glycerol hydrogenolysis is an important parameter in gaining high product selective *i.e.*, 1,3-PDO was studied. As we know, the contact time decreases by increasing the feed flow rate. It is crucial to optimise the H₂ reactant flow to reduce the operating cost and avoid the successive hydrogenated by-products formation. In Fig. 7 illustrates the effect of contact times on glycerol conversion and product selectivity. In this case, the contact time is changed with the hydrogen flow rates (W/F_{tot}). As predicted, the activity increased with contact time and this effect is evident from H₂ flow rate point of view (whereas glycerol and weight of the catalyst is constant). It can be noticed that the glycerol conversion enhanced linearly from 69 to 90% with contact times *i.e.*, H₂ flowrates form 10 mL min⁻¹ to 50 mL min⁻¹. Henceforth, the activity increased by with contact times and lowering the H₂ flow rates, similar trend was observed by Samudrala et al., 2018 [14, 19]. The selectivity of 1,3-PDO increased from 36 to 51% with hydrogen flow rate and further increment in hydrogen flow rate *i.e.*, above 30 mL min⁻¹ will decrease the selectivity of 1,3-PDO [32]. However, hydrogen flow rate over 30 mL min⁻¹ leads to an increase in the propanols selectivity, probably due to the increased concentration of

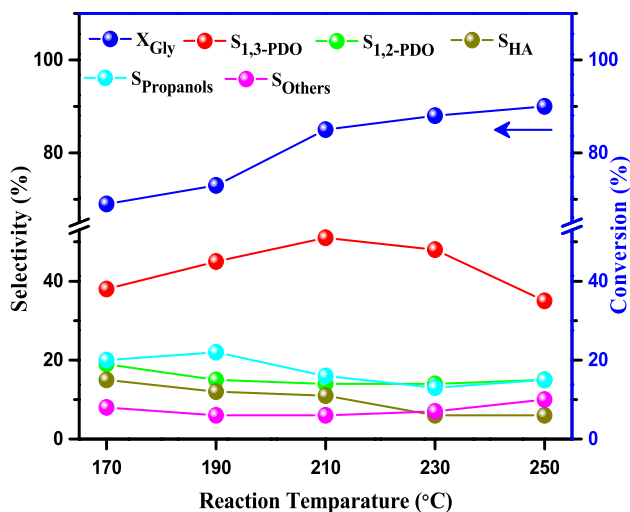


Fig. 6 Effect of reaction temperature on hydrogenolysis of glycerol to propanediols. Reaction conditions: 0.5 g catalyst, Reaction temperature: 170–210 °C, H₂ flow rate: 30 mL min⁻¹, WHSV-2.37 h⁻¹, 1,3-propanediol (S_{1,3-PDO}), 1,2-propanediol (S_{1,2-PDO}); Hydroxyacetone (S_{HA}), 1-Propanol, 2-Propanol (S_{Propanol})

H⁺ and H⁻ over the catalyst surface and promotes successive hydrogenation activity steps. In this reaction, hydrogen is an excessive reactant and probably follows a pseudo first-order reaction kinetics with respect to glycerol concentration.

Effect of WHSVs

The influence of weight hourly space velocity (WHSV) on glycerol hydrogenolysis reaction over 2Pt-10WO₃/TiP catalyst at 210 °C was studied by varying the catalyst weight from 0.2 to 0.6 g and the results are presented in Fig. 8. The results in Fig. 8 reflect the conversion of glycerol decreased with WHSVs, as predicted, increased feed flow rates declined the activity due to limited active sites. Moreover, activity enhanced with catalyst weight and attained better results at 0.5 g which is the most appropriate catalyst mass to gained highest selectivity and conversion. At low WHSV 2.37 h⁻¹ is the optimal for gaining the highest activity *i.e.*, high conversion and selectivity. Moreover, the glycerol concentration was also studied and the best selectivity of 1,3-PDO was achieved with 10 wt.% glycerol feed. The glycerol conversion decreased with increased in the glycerol concentration. As predicted, a high conversion and selectivity will be achieved at low reactant concentration and this similar phenomenon was reported in [14, 19]. At high concentrations *i.e.*, above 10 wt.%, excessive unreacted glycerol was formed due to non-availability of active sites and lead to low reaction rates [19]. The glycerol conversion and selectivity to 1,3-PDO declines relatively at 15 and 20 wt.%. Overall, the glycerol reactant concentration of 10 wt.% is the most optimized value in obtaining the highest activity.

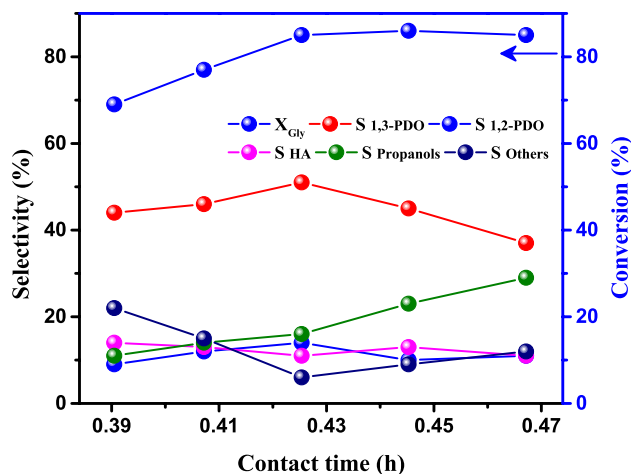


Fig. 7 Effect of contact times on hydrogenolysis of glycerol to propanediols. Reaction conditions: 0.2–0.5 g catalyst, reaction temperature: 210 °C, H₂ flow rate: 10 to 50 mL min⁻¹, 1,3-propanediol (S_{1,3-PDO}), 1,2-propanediol (S_{1,2-PDO}), hydroxyacetone (S_{HA}), 1-Propanol, 2-Propanol (S_{Propanol})

Time on stream (TOS)

The activity results from gas phase hydrogenolysis of glycerol over 2Pt-10WO₃/TiP catalyst at 210 °C reaction are shown in Fig. 9. Both the glycerol conversion and 1,3-PDO selectivity increased with reaction time and reached a maximum conversion of 85% and selectivity of 51% was achieved after 4 h time on stream (TOS). After reaching maximum activity in terms of conversion and selectivity after 4 h, the activity starts to decline. A relative drop in activity trend was visible after 4 h, probably due to catalyst deactivation

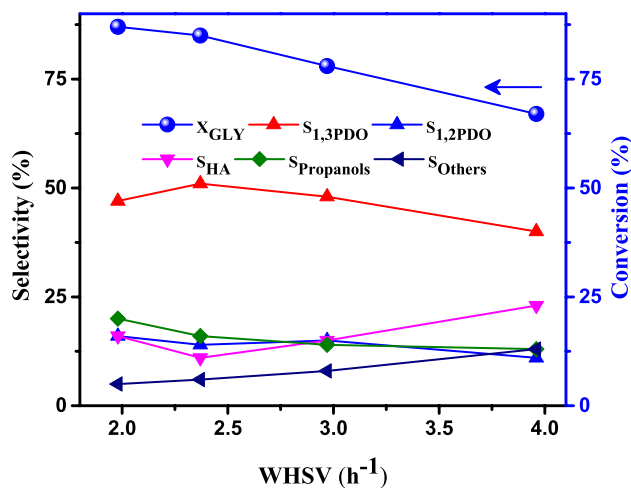


Fig. 8 Effect of WHSV on hydrogenolysis of glycerol to propanediols. Reaction conditions: 0.2–0.5 g catalyst, Reaction temperature: 210 °C, H₂ flow rate: 30 mL min⁻¹, 1,3-propanediol (S_{1,3-PDO}), 1,2-propanediol (S_{1,2-PDO}), Hydroxyacetone (S_{HA}), 1-Propanol, 2-Propanol (S_{Propanol})

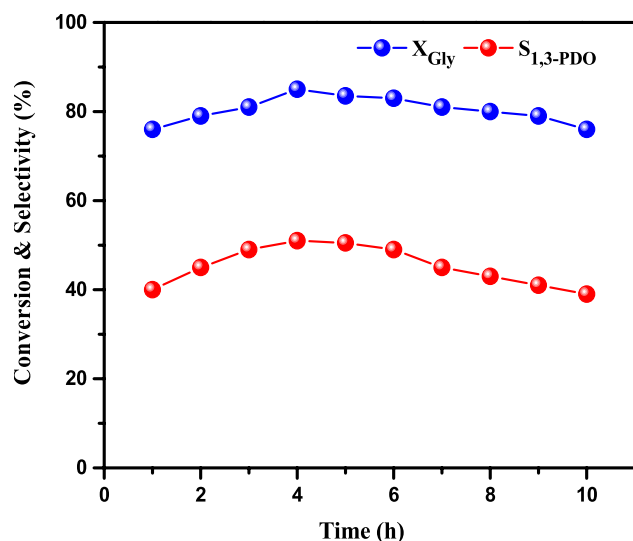


Fig. 9 Time on stream for hydrogenolysis of glycerol to 1,3-PDO. Reaction conditions: 0.5 g catalyst, Reaction temperature: 210 °C, H₂ flow rate: 30 mL min⁻¹

by carbon formation over the catalyst surface. The carbon coke formation during glycerol hydrogenolysis was confirmed by the CHNO analysis (Table 4). The time on stream results confirm that the catalyst is relatively unstable for a long period of time.

Comparison of the present work with those published data on state of the art in Table 4 was summarized. The Pt-WO_x active phase and W promoter are widely studied over different support materials. However, the stability of the catalysts is not reported widely in the literature. In this work, we exclusively introduced TiP based support, which is quite novel approach. The reported catalyst performances

are typically high and found some discrepancies. However, it is hard to compare with those literature articles due to many factors. We compared some of them most active catalysts which are similar to Pt/WO_x combinations at different reaction conditions. The structure-acidity, active phase-activity and acidity-activity are typical correlations made in this Table. Overall, the WO_x content had a major effect on the final catalytic properties [24, 33, 34].

Deactivation Studies

The spent catalyst 2Pt-10WO₃/TiP was characterized by NH₃-TPD and BET surface area and the results are compared with those of fresh catalyst (Table 5). The spent catalyst was first pretreated under air flow at 300 °C for 3 h and then reduced under H₂ flow at 300 °C for 2 h to regenerate the activity and the catalyst reusability. The reaction was repeated with a regenerated catalyst under similar reaction conditions. The used catalyst was characterized to understand the changes in physicochemical properties undergone during glycerol hydrogenolysis reaction, and the results are shown in Table 5. Activity results of spent catalyst were performed, and the conversion and selectivity declined from 85 to 81% and 51% to 48%, linearly with TOS. The instability of the catalyst is due to the deactivation caused by carbon formation. The acidity and BET surface area values of the spent catalyst was found to be decreased compared to the fresh catalyst due to agglomeration of Pt particles as well as carbon coke formation, which is evident by CHNO analysis. Further studies will be conducted to improve the catalyst stability by understanding the phenomena of carbon formation and also by introducing the promoters and modifying the reaction conditions (to avoid the carbon formation).

Table 4 List of Pt-based catalysts reported in literature on glycerol hydrogenolysis to 1,3-PDO

Catalyst	Reaction conditions	Conversion (%)	1,3-PDO Selectivity (%)	Reference
2Pt-10WO ₃ /SBA-15	T=210 °C, p _{H2} =0.1 MPa, WHSV = 1.02 h ⁻¹ , C _{glycerol} = 10 wt.%, FBR	86	42	[24]
Pt/5WO ₃ /10TiO ₂ /SiO ₂	T=180 °C, p _{H2} =5.5 MPa, t=12 h, C _{glycerol} = 10 wt.%, BR	15	51	[33]
Pt/WO _x /AlOOH	T=140 °C, p _{H2} =0.5 MPa, t=12 h, C _{glycerol} = 10 mmol _{glycerol} , BR	37	21	[34]
Pt/WO ₃ /Al ₂ O ₃	T=260 °C, WHSV=0.14 h ⁻¹ , C _{glycerol} =20 wt.%, FBR	99	14	[35]
9Pt/8WO ₃ /Al ₂ O ₃	T=200 °C, p _{H2} =90 bar, t=4 h, C _{glycerol} =20 wt.%, BR	80	39	[36]
2Pt-10WO ₃ /SBA-15	T=210 °C, p _{H2} =0.1 MPa, WHSV = 1.02 h ⁻¹ , C _{glycerol} = 10 wt.%, FBR	86	42	[24]
2Pt/20(W + Al)-SBA-15	T=160 °C, p _{H2} =6 MPa, t=12 h, C _{glycerol} = 3 wt.%, BR	66	50	[37]
6Pt/12.9 W/Al ₂ O ₃	T=180 °C, p _{H2} =5 MPa, WHSV = 1 h ⁻¹ , C _{glycerol} = 50 wt.%, FBR	80	35	[38]
Pt/S-MMT	T=200 °C, p _{H2} =0.1 MPa, WHSV = 1.02 h ⁻¹ , C _{glycerol} = 10 wt.%, FBR	94	62	[14]
2Pt-10 WO ₃ /TiP	T=210 °C, p _{H2} =0.1 MPa, t=4 h, C _{glycerol} = 10 wt.%, FBR	85	51	This work

T reaction temperature, p_{H2} hydrogen partial pressure, WHSV weight hour space velocity, t time on stream, C_{glycerol} glycerol concentration, FBR fixed bed reactor, BR batch reactor

Table 5 Activity results and the properties of spent catalyst 2Pt-10WO₃/TiP

Catalyst	X _{GLY} (%)	S _{1,3-PDO} (%)	BET surface area ^a (m ² /g)	Total acidity ^b (μmol/g)	C ^c (%)
2Pt-10WO ₃ /TiP (fresh)	85	51	165.2	210	0.08
2Pt-10WO ₃ /TiP (spent)	81	48	152.3	193	3.51

^aBET surface area^bNH₃-TPD^cCHNO analysis

Conclusion

In summary, we prepared and modified a bifunctional Pt-WO₃ supported TiP (titanium phosphate) based catalysts using hydrothermal synthesis and wet impregnation methods. The effect of Pt and WO₃ loadings were studied in the vapour phase hydrogenolysis of glycerol. The addition of WO₃ to Pt-based catalysts significantly improved the selectivity toward 1,3-PDO formation via direct glycerol hydrogenolysis. The profound effects were found in chemical and physical variations of the final catalytic properties after the incorporation of Pt and WO₃ into the TiP framework. The coordination of WO₃ with TiP structure led to creation of active sites via incorporation of Brønsted acidity. In comparison to WO₃/TiP catalyst, the bifunctional Pt-WO₃/TiP catalyst (optimal: Pt = 2 wt.% & WO₃ = 10 wt.%) exhibited a highest glycerol conversion of 85% and 1,3-PDO selectivity of 51% at 210 °C. The high performance of 2Pt-10WO₃/TiP is owing to its salient features in terms of highest total acidity, good Pt dispersion, high active surface area, and strong interactions between Pt-WO₃ (confirmed from TPD, FTIR, TEM and XRD analysis). However, the catalyst gained highest activity in terms of glycerol conversion and 1,3-PDO at 4 h reaction time, thereafter, the activity drops linearly with TOS. The catalyst 2Pt-10WO₃/TiP was found to be unstable after 4 h TOS due to deactivation occurred via carbon formation. In the future, improving the catalyst stability will be considered by understanding the mechanism of carbon formation.

Supplementary Information The online version contains supplementary material available at <https://doi.org/10.1007/s12649-022-01909-4>.

Acknowledgements The authors PB thanks University Grants Commission (UGC), New Delhi, for the award of Senior Research Fellowship.

Funding Open Access funding provided by University of Oulu including Oulu University Hospital. Dr. Putra Kumar acknowledges the funding and research support from IICT Hyderabad and CSIR, Delhi, India. Dr. Prem Kumar Seelam acknowledges and is thankful to the project Hycat2 and Hycamite Oy, Kokkola, Finland.

Data Availability All data used in this manuscript are generated and analysed during the experimental studies. Different data is generated during the materials characterisation and activity tests. Most of the data are included and presented in the form of figures, graphical and tabular columns in this manuscript. The raw data is available in excel and other formats. Upon requests for the additional material should be made to the corresponding authors.

Declarations

Conflict of interest The authors declare no conflicts of interest.

Open Access This article is licensed under a Creative Commons Attribution 4.0 International License, which permits use, sharing, adaptation, distribution and reproduction in any medium or format, as long as you give appropriate credit to the original author(s) and the source, provide a link to the Creative Commons licence, and indicate if changes were made. The images or other third party material in this article are included in the article's Creative Commons licence, unless indicated otherwise in a credit line to the material. If material is not included in the article's Creative Commons licence and your intended use is not permitted by statutory regulation or exceeds the permitted use, you will need to obtain permission directly from the copyright holder. To view a copy of this licence, visit <http://creativecommons.org/licenses/by/4.0/>.

References


1. Balla, P., Seelam, P.K., Balaga, R., Rajesh, R., Perupogu, V., Liang, T.X.: Immobilized highly dispersed Ni nanoparticles over porous carbon as an efficient catalyst for selective hydrogenation of furfural and levulinic acid. *J. Environ. Chem. Eng.* **9**, 106530 (2021). <https://doi.org/10.1016/j.jece.2021.106530>
2. Saeidabad, N.G., Noh, Y.S., Eslami, A.A., Song, H.T., Kim, H.D., Fazeli, A., Moon, D.J.: A review on catalysts development for steam reforming of biodiesel derived glycerol; promoters and supports. *Catalysts* **10**, 1–22 (2020). <https://doi.org/10.3390/catal10080910>
3. Singh, G., Pradhan, G., Pradhan, S., Sharma, Y.C.: Transformation of biodiesel waste glycerol to value added glycerol carbonate. *Chem Sci Rev Lett* **9**, 1003–1013 (2020)
4. Carlucci, C.: A focus on the transformation processes for the valorization of glycerol derived from the production cycle of biofuels. *Catalysts* **11**, 1–24 (2021). <https://doi.org/10.3390/catal11020280>
5. Xi, Z., Jia, W., Zhu, Z.: WO₃-ZrO₂-TiO₂ composite oxide supported Pt as an efficient catalyst for continuous hydrogenolysis of glycerol. *Catal. Lett.* (2020). <https://doi.org/10.1007/s10562-020-03270-4>

6. Quispe, C.A.G., Coronado, C.J.R., Carvalho, J.A.: Glycerol: Production, consumption, prices, characterization and new trends in combustion. *Renew. Sustain. Energy Rev.* **27**, 475–493 (2013). <https://doi.org/10.1016/j.rser.2013.06.017>
7. Lei, N., Miao, Z., Liu, F., Wang, H., Pan, X., Wang, A., Zhang, T.: Understanding the deactivation behavior of Pt/WO₃/Al₂O₃ catalyst in the glycerol hydrogenolysis reaction, *Chinese J. Catal.* **41**, 1261–1267 (2020). [https://doi.org/10.1016/S1872-2067\(20\)63549-5](https://doi.org/10.1016/S1872-2067(20)63549-5)
8. Bhowmik, S., Enjamuri, N., Darbha, S.: Hydrogenolysis of glycerol in an aqueous medium over Pt/WO₃/zirconium phosphate catalysts studied by ¹H NMR spectroscopy. *New J. Chem.* **45**, 5013–5022 (2021). <https://doi.org/10.1039/d0nj05557c>
9. Mitta, H., Seelam, P.K., Ojala, S., Keiski, R.L., Balla, P.: Tuning Y-zeolite based catalyst with copper for enhanced activity and selectivity in vapor phase hydrogenolysis of glycerol to 1,2-propanediol. *Appl. Catal. A Gen.* **550**, 308–319 (2018). <https://doi.org/10.1016/j.apcata.2017.10.019>
10. Mitta, H., Devunuri, N., Sunkari, J., Mutyala, S., Balla, P., Perupogu, V.: A highly active dispersed copper oxide phase on calcined Mg₉Al₂.7-Ga₂.3O₂ catalysts in glycerol hydrogenolysis. *Catal. Today.* **375**, 204–215 (2021). <https://doi.org/10.1016/j.cattod.2020.02.032>
11. Kumar, V.P., Harikrishna, Y., Nagaraju, N., Chary, K.V.R.: Characterization and reactivity of TiO₂ supported nano ruthenium catalysts for vapour phase hydrogenolysis of glycerol. *Indian J. Chem.* **53**, 516–523 (2014)
12. Shinmi, Y., Koso, S., Kubota, T., Nakagawa, Y., Tomishige, K.: Modification of Rh/SiO₂ catalyst for the hydrogenolysis of glycerol in water. *Appl. Catal. B Environ.* **94**, 318–326 (2010). <https://doi.org/10.1016/j.apcatb.2009.11.021>
13. Priya, S.S., Bhanuchander, P., Kumar, V.P., Dumbre, D.K., Periasamy, S.R., Bhargava, S.K., Lakshmi Kantam, M., Chary, K.V.R.: Platinum supported on H-mordenite: a highly efficient catalyst for selective hydrogenolysis of glycerol to 1,3-propanediol. *ACS Sustain. Chem. Eng.* **4**, 1212–1222 (2016). <https://doi.org/10.1021/acsschemeng.5b01272>
14. Samudrala, S.P., Kandasamy, S., Bhattacharya, S.: Turning biodiesel waste glycerol into 1,3-propanediol: catalytic performance of sulphuric acid-activated montmorillonite supported platinum catalysts in glycerol hydrogenolysis. *Sci. Rep.* **8**, 1–12 (2018). <https://doi.org/10.1038/s41598-018-25787-w>
15. Tomishige, K., Tamura, M., Nakagawa, Y.: Role of Re species and acid cocatalyst on Ir-ReOx/SiO₂ in the C-O hydrogenolysis of biomass-derived substrates. *Chem. Rec.* **14**, 1041–1054 (2014). <https://doi.org/10.1002/tcr.201402026>
16. Liu, L., Asano, T., Nakagawa, Y., Tamura, M., Okumura, K., Tomishige, K.: Selective hydrogenolysis of glycerol to 1,3-propanediol over rhenium-oxide-modified iridium nanoparticles coating rutile titania support. *ACS Catal.* (2019). <https://doi.org/10.1021/acscatal.9b03824>
17. Liu, L., Kawakami, S., Nakagawa, Y., Tamura, M., Tomishige, K.: Highly active iridium-rhenium catalyst condensed on silica support for hydrogenolysis of glycerol to 1,3-propanediol. *Appl. Catal. B Environ.* **256**, 117775 (2019). <https://doi.org/10.1016/j.apcatb.2019.117775>
18. Priya, S.S., Bhanuchander, P., Kumar, V.P., Bhargava, S.K., Chary, K.V.R.: Activity and selectivity of platinum-copper bimetallic catalysts supported on mordenite for glycerol hydrogenolysis to 1,3-propanediol. *Ind. Eng. Chem. Res.* **55**, 4461–4472 (2016). <https://doi.org/10.1021/acs.iecr.6b00161>
19. Samudrala, S.P.: Toward the sustainable synthesis of propanols from renewable glycerol over MoO₃-Al₂O₃ supported palladium catalysts. *Catalysts.* (2018). <https://doi.org/10.3390/catal8090385>
20. Zhu, M., Chen, C.: Oxides supported platinum catalyst. *React. Kinet. Mech. Catal.* **124**, 683–699 (2018). <https://doi.org/10.1007/s11144-018-1379-z>
21. Aihara, T., Miura, H., Shishido, T.: Investigation of the mechanism of the selective hydrogenolysis of C O bonds over a Pt/WO₃/Al₂O₃ catalyst. *Catal. Today.* **352**, 73–79 (2020). <https://doi.org/10.1016/j.cattod.2019.10.008>
22. Zhou, W., Luo, J., Wang, Y., Liu, J., Zhao, Y., Wang, S., Ma, X.: WOx domain size, acid properties and mechanistic aspects of glycerol hydrogenolysis over Pt/WOx/ZrO₂. *Appl. Catal. B Environ.* **242**, 410–421 (2019). <https://doi.org/10.1016/j.apcatb.2018.10.006>
23. da Silva Ruy, A.D., de Brito Alves, R.M., Reis Hewer, T.L., de Aguiar Pontes, D., Gomes Teixeira, L.S., Magalhães Pontes, L.A.: Catalysts for glycerol hydrogenolysis to 1,3-propanediol: a review of chemical routes and market. *Catal. Today.* **381**, 243–253 (2021). <https://doi.org/10.1016/j.cattod.2020.06.035>
24. Priya, S.S., Kumar, V.P., Kantam, M.L., Bhargava, S.K., Srikanth, A., Chary, K.V.R.: High efficiency conversion of glycerol to 1,3-propanediol using a novel platinum-tungsten catalyst supported on SBA-15. *Ind. Eng. Chem. Res.* **54**, 9104–9115 (2015). <https://doi.org/10.1021/acs.iecr.5b01814>
25. Zhu, S., Qiu, Y., Zhu, Y., Hao, S., Zheng, H., Li, Y.: Hydrogenolysis of glycerol to 1,3-propanediol over bifunctional catalysts containing Pt and heteropolyacids. *Catal. Today.* **212**, 120–126 (2013). <https://doi.org/10.1016/j.cattod.2012.09.011>
26. Bhaumik, A., Inagaki, S.: Mesoporous titanium phosphate molecular-sieves with ion-exchange capacity. *J. Am. Chem. Soc.* **123**, 691–696 (2001). <https://doi.org/10.1021/ja002481s>
27. Bhanuchander, P., Samudrala, S.P., Putrakumar, B., Vijayanand, P., Kumar, B.S., Chary, K.V.R.: Hydrogenation of levulinic acid to valeric acid over platinum-tungsten catalysts supported on γ-Al₂O₃. *New J. Chem.* **43**, 18003–18011 (2019). <https://doi.org/10.1039/c9nj04056k>
28. Fei, H., Zhou, X., Zhou, H., Shen, Z., Sun, P., Yuan, Z., Chen, T.: Facile template-free synthesis of meso-macroporous titanium phosphate with hierarchical pore structure. *Microporous Mesoporous Mater.* **100**, 139–145 (2007). <https://doi.org/10.1016/j.micromeso.2006.10.019>
29. Jarauta-Córdoba, C., Bengoechea, M.O., Agirrezabal-Telleria, I., Arias, P.L., Gandarias, I.: Insights into the nature of the active sites of pt-wox/al₂o₃ catalysts for glycerol hydrogenolysis into 1,3-propanediol. *Catalysts* **11**, 1–16 (2021). <https://doi.org/10.3390/catal11101171>
30. Yang, X.L., Dai, W.L., Gao, R., Fan, K.: Characterization and catalytic behavior of highly active tungsten-doped SBA-15 catalyst in the synthesis of glutaraldehyde using an anhydrous approach. *J. Catal.* **249**, 278–288 (2007). <https://doi.org/10.1016/j.jcat.2007.05.002>
31. Wang, Y., Zhou, J., Guo, X.: Catalytic hydrogenolysis of glycerol to propanediols: a review. *RSC Adv.* **5**, 74611–74628 (2015). <https://doi.org/10.1039/c5ra11957j>
32. Nakagawa, Y., Tamura, M., Tomishige, K.: Catalytic materials for the hydrogenolysis of glycerol to 1,3-propanediol. *J. Mater. Chem. A* **2**, 6688–6702 (2014). <https://doi.org/10.1039/c3ta15384c>
33. Gong, L., Lu, Y., Ding, Y., Lin, R., Li, J., Dong, W., Wang, T., Chen, W.: Selective hydrogenolysis of glycerol to 1,3-propanediol over a Pt/WO₃/TiO₂/SiO₂ catalyst in aqueous media. *Appl. Catal. A Gen.* **390**, 119–126 (2010). <https://doi.org/10.1016/j.apcata.2010.10.002>
34. Utraporn, P., Praserttham, P.: Effect of calcination temperature and support type of Pt/WOx/boehmite catalyst on 1,3-propanediol production from hydrogenolysis of glycerol. *IOP Conf. Ser. Mater. Sci. Eng.* (2019). <https://doi.org/10.1088/1757-899X/559/1/012012>

35. Edake, M., Dalil, M., Darabi Mahboub, M.J., Dubois, J.L., Patience, G.S.: Catalytic glycerol hydrogenolysis to 1,3-propanediol in a gas-solid fluidized bed. *RSC Adv.* **7**, 3853–3860 (2017). <https://doi.org/10.1039/c6ra27248g>
36. García-Fernández, S., Gandarias, I., Requies, J., Soulimani, F., Arias, P.L., Weckhuysen, B.M.: The role of tungsten oxide in the selective hydrogenolysis of glycerol to 1,3-propanediol over Pt/WO_x/Al₂O₃. *Appl. Catal. B Environ.* **204**, 260–272 (2017). <https://doi.org/10.1016/j.apcatb.2016.11.016>
37. Feng, S., Zhao, B., Liang, Y., Liu, L., Dong, J.: Improving selectivity to 1,3-propanediol for glycerol hydrogenolysis using W- and Al-incorporated SBA-15 as support for Pt nanoparticles. *Ind. Eng. Chem. Res.* **58**, 2661–2671 (2019). <https://doi.org/10.1021/acs.iecr.8b03982>
38. Lei, N., Zhao, X., Hou, B., Yang, M., Zhou, M., Liu, F., Wang, A., Zhang, T.: Effective hydrogenolysis of glycerol to 1,3-propanediol over metal-acid concerted Pt/WO_x/Al₂O₃ catalysts. *ChemCatChem* **11**, 3903–3912 (2019). <https://doi.org/10.1002/cctc.201900689>

Publisher's Note Springer Nature remains neutral with regard to jurisdictional claims in published maps and institutional affiliations.

Authors and Affiliations

Bhanuchander Ponnala¹ · Putrakumar Balla¹ · S. K. Hussain¹ · Srinivasa Rao Gijnjupalli² · Kumaraswamy Koppadi¹ · Nagaraju Nekkala¹ · Vijayanand Perupogu¹ · Ulla Lassi³ · Prem Kumar Seelam³ 

¹ Energy and Environmental Engineering Department, CSIR-Indian Institute of Chemical Technology, Hyderabad, Telangana 500007, India

² Department of Applied Science, University of Technology and Applied Science, 74, Muscat, Sultanate of Oman

³ Sustainable Chemistry Research Unit, Faculty of Technology, University of Oulu, P.O. Box 4300, 90014 Oulu, Finland